Transactions on Biomedicine and Health vol 2, © 1995 WIT Press, www.witpress.com, ISSN 1743-3525

Self-sustaining spiral wave activity in a two-dimensional ionic model of cardiac ventricular muscle

J. Beaumont, N. Davidenko, J. Davidenko, J. Jalife
Department of Pharmocology, State University of New York, Health Science Center, Syracuse, NY 13210, USA

1 Introduction

Recent experiments in isolated heart muscle preparations have demonstrated that relatively small pieces of 2-dimensional anisotropic myocardium (2 cm x 2 cm x 0.5 mm) can sustain electrical rotors radiating spiral waves of activity [5]. Spiral waves are initiated using cross field stimulation [5] and may be sustained and stable for long periods of time (beyond 20 min.). The organizing center of the spiral (i.e, the rotor or "core") is usually $\approx$ 3 x 5 mm, the rotation period ranges between 100 and 200 msec, and the action potential duration ranges between 80 and 150 msec during fast stimulation frequency. We have carried out computer simulations using a membrane model that incorporates the main ionic currents of the ventricular cell to simulate spiral wave activity in 2-D cardiac muscle. Our long-term objective is to identify the ionic mechanisms associated with the establishment of sustained electrical rotors. Previous computer simulations have questioned the ability to obtain sustain spiral wave activity in 2-D models that simulate small healthy preparations [4]. Here we have used Phase I of the Luo and Rudy (LR) model [7] to demonstrate that under appropriate parametric conditions, involving a slight modification in the kinetics of the activation front, it is possible to induce stable spiral waves that are sustained for long periods of time. In addition, we provide an account of our revision of the model formulation for the sodium current, which led to the ability of the LR model to reproduce spiral wave behavior as observed experimentally in isolated preparations of heart muscle.

Table 1. Variables of the Hodgkin-Huxley equations.

variable	definition	unit
u(x,t):	membrane potential	mV
C_p :	membrane capacitance (1 for cardiac cells)	$\mu F/cm^2$
υ :	volume-to-surface ratio of the medium	cm
D:	tensor of diffusion	$(K\Omega\, cm)^{-1}$
$Iion_s(u,t)$:	ionic current of a species s	$\mu A/cm^2$
$I_0(x,t)$:	current stimulus	$\mu A/cm^2$
$\bar{g}_s(u)$:	maximal conductance of a channel s	mS/cm^2
E_s :	reversal potential of an ionic current s	mV
$y_{k,s}(u,t)$:	fraction of gates k in the open state	no unit
$Y_{k,s}(u)$:	steady state of a gating variable $y_{k,s}$	no unit
$\lambda_{k,s}$:	number of molecular particles in a gate	no unit
$\tau_{k,s}(u)$:	time constant of a gate	msec

2 Model Formulation

Equations of the system

The basis for the equations of propagation of electrical impulses in cardiac muscle is the conservation of charge; in the case in which the cardiac cell membrane is treated as a passive resistance, the equation is similar to the heat equation. For excitable cells the passive term is replaced by the non-linear equations governing the current flux across the membrane, which in our study are the Hodgkin- Huxley (HH) equations. We write the system of equations in a general form as follows:

$$-C_p\frac{\partial u}{\partial t} + \upsilon\,\nabla \bullet (D\nabla u) = \sum_s Iion_s(u,t) + I_0(x,t) \quad (1)$$

$$Iion_s(u,t) = \bar{g}_s(u)\left(\prod_k y_k^{\lambda_k}(u,t)\right)_s (u - E_s) \quad (2)$$

$$\frac{dy_{k,s}(u,t)}{dt} = \frac{(Y_{k,s}(u) - y_{k,s}(u,t))}{\tau_{k,s}(u)} \quad (3)$$

The meaning of each system variable is presented in Table 1. In this article the derivatives relative to time are noted with a subscript t or with a dot above the variable. The variable x is a vector where its components (x_0, x_1) stand for the orthogonal axis of the system. Although the general formulation above (eqns. 1-3) encompasses most of the membrane models, there are some deviations (e.g. the reversal potential is a function of the current). In the present study we do not consider such cases. The functions $Y(u)$, $\tau(u)$ and $\bar{g}(u)$ are smooth and the function $Y(u)$ is monotonic and bounded between 0 and 1.

Spatial discretization

To simplify, we write equation (1) as follows (we intentionally omit C_p):

$$-u_t + A\,u = \mathcal{I}(u) \quad \text{on } \Phi \tag{4}$$

With the boundary and initial conditions:

$$\frac{\partial u}{\partial \nu} = 0 \quad \text{on } \Gamma\text{x}[0,\text{T}] \tag{5}$$

$$u(x,0) = u_0(x) \qquad \text{on } \Phi \tag{6}$$

$$y_{k,s}(x,0) = Y_{k,s}(u(x,0)) \qquad \text{on } \Phi \tag{7}$$

Φ is the domain of interest, Γ is its boundary and ν is a vector pointing in the outward direction normal to the boundary. I_0, the current stimulus, is a pulse in space and time. Let the set of functions ϕ_n be a basis in the Hilbert space $\mathcal{H}^d$. We obtain a numerical solution of the differential equation (4-7) by requiring that the vector $u_t - (Au - \mathcal{I}(u))$ be orthogonal to all of the functions ϕ_n of the basis (Galerkin method):

$$< u_t, \phi_n > + < Au, \phi_n > = < \mathcal{I}(u), \phi_n > \tag{8}$$

$$< u_t, \phi_n > = \int_\Phi u_t\,\phi_n\,dx$$

$$< Au, \phi_n > = \int_\Phi Au\,\phi_n\,dx$$

$$< \mathcal{I}(u), \phi_n > = \int_\Phi \mathcal{I}(u)\,\phi_n\,dx$$

Applying Green's formula to the term $< Au, \phi >$ in eqn. (8), using the fact that $\partial u/\partial \nu = 0$ on Γ and, approximating u in the above relations by a linear combination of the functions $\phi_n(x)$ of the basis, one obtains an N x N matrix system ([11, chap. 3-4]):

$$Q\,\dot{C} + K\,C = F(U) \tag{9}$$

Where C is the vector of coefficients c_n of the linear combination of functions ϕ_n, Q and K (mass and stiffness matrices) are NxN matrices which are solely dependent on the geometry of the system and F(u) is a vector (force vector) that depends on the ionic currents at a particular time. In this work, we used a Lagrange family of interpolation polynomials of degree $d \geq 1$, defined on rectangular elements of the discretized domain Φ [11, chap. 4]. We have developed software that enables us to build a matrix system when the basis of functions is composed of Lagrange polynomials of any degree.

Discretization in time

By projecting the vector $u_t - (A\,u - \mathcal{I}(u))$ in the finite dimensional space (in the Hilbert sense) composed of the functions ϕ_n, we transformed the partial differential equation (PDE;8) to an ordinary differential equation (ODE;9). Since we are using a Lagrange family of interpolation polynomials,

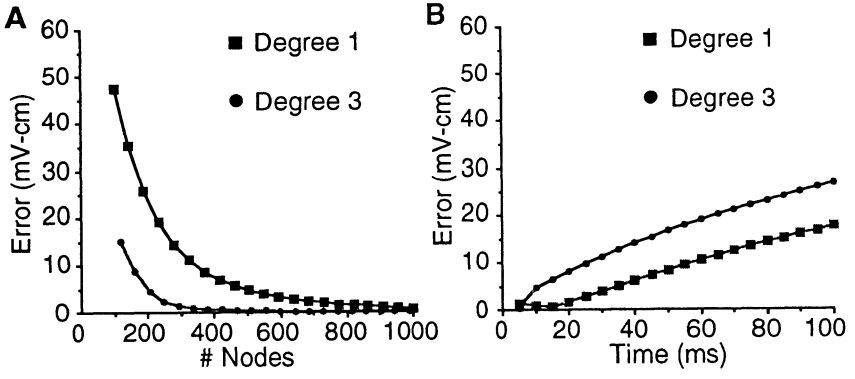


Figure 1: Convergence tests for the numerical calculation of the traveling wave solution of the Hodgkin-Huxley equations.

the vector C in (9) is replaced by the vector U, the components of which are given by the function $u(x,t)$, sampled at the global nodes of Φ [11]. We solve the ODE (9) with a semi- implicit time scheme. We introduce the index z which refers to a particular sample in time, $t_z = \sum_{i=1}^{z} \Delta t_z$, Δt_z being the time step. In a finite difference scheme, $\frac{\Delta U}{\Delta t} = \gamma \dot{U}_{z+1} + (1-\gamma)\dot{U}_z$. For $\gamma = 0$, the integration time scheme is explicit and is implicit for any other values. In addition, for $\gamma = 1/2$ the rate of convergence is quadratic. Combining this expression with eqn. (9), we obtain the following relation for U_{z+1}:

$$\begin{aligned} R_2 U_{z+1} &= R_1 U_z + R_0 \\ R_2 &= Q + \gamma \Delta t K \\ R_1 &= Q - (1-\gamma)\Delta t K \\ R_0 &= \Delta t (\gamma F(U_{z+1}) + (1-\gamma) F(U_z)) \end{aligned} \tag{10}$$

For the first iteration on an interval of time, we set $U_z = U_{z+1}$ in the last line of eqn. (10) and use the value of the previous iteration for U_{z+1} in all subsequent iterations. For each iteration, $\gamma = 1/2$. The values of the gating variables are updated using a fully implicit integration scheme of the Crank- Nicolson type:

$$y_{z+1} = \frac{y_z \left(1 - \frac{\Delta t_z}{2\tau(u_z)}\right) + \frac{\Delta t_z}{2}\left(\frac{Y(u_z)}{\tau(u_z)} + \frac{Y(u_{z+1})}{\tau(u_{z+1})}\right)}{1 + \frac{\Delta t_z}{2\tau(u_z)}} \tag{11}$$

The scheme is obtained from a discretization of the derivative in eqn. (3) with $\gamma = 1/2$ and assuming that $u(x,t)$ is known at t and $t + dt$. The matrix system 10 is solved with a preconditioned (SSOR technique) conjugate gradient technique [1].

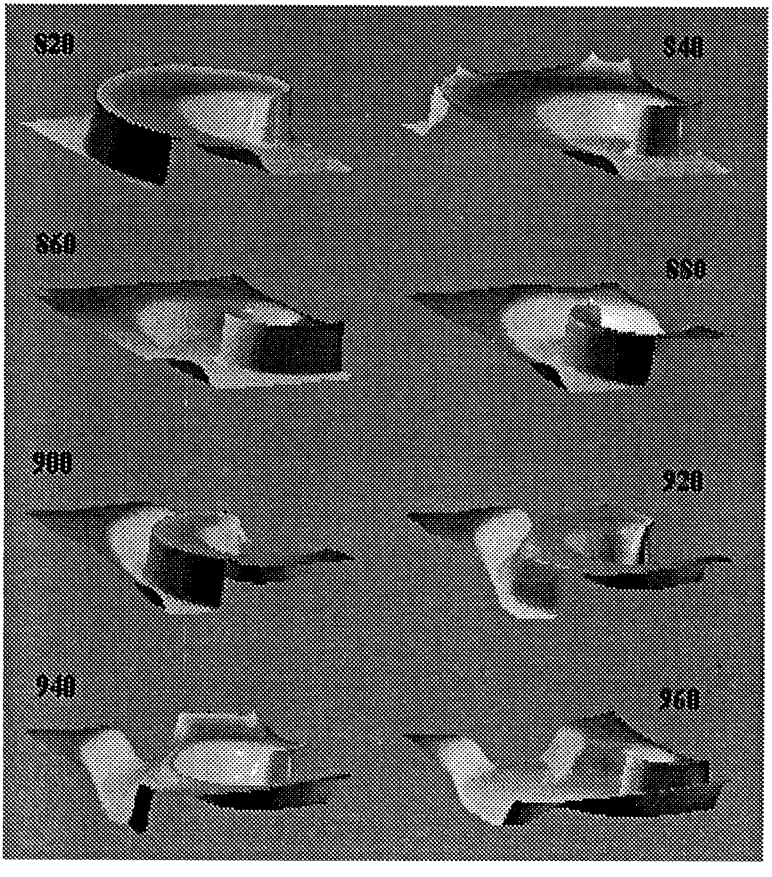


Figure 2: Spiral wave activity on an isotropic cardiac muscle of 4 cm x 4 cm.

3 Simulation Results

Convergence tests

We first compare numerical solutions obtained in a cable when using varying space and time steps. For these tests, we use Phase I of the LR model [7]; i.e. the functions in eqns. (1-3) are specified by this model (note that E_{si} was fixed to 80 mV). The test configuration is a cable, 2 cm long, and has an axial resistivity of 200 Ωcm. The electrical impulse is initiated by a stimulus of 15 $\mu A/cm^2$ in strength and 5 msec in duration, applied uniformly from 0 to 2 mm. The difference between two potential distributions was estimated by measuring the distance between two functions in the L_2 norm. A control solution was calculated using polynomials of degree 5, an internode spacing of 20 μm (200 elements for a cable of 2 cm long) and a time step of 100

μsec. In panel A of Figure 1 we show the error obtained when only the space step between the nodes is changed using polynomials of degrees 1 and 3 (distance is always measured with respect to the control solution). In panel B of the same Figure we show the error at different instants in time for a test solution using an internode spacing of 100 μm for polynomials of degree 1, and 67 μm for polynomials of degree 3. In both cases the space step was 100 μsec. For this test the cable was 14 cm long. We also determined the error when only the space step was changed. For time steps of 5, 50 and 100 μsec, the errors were 0.533, 2.396 and 7.215 $mV\,cm$ for polynomials of degree 1 and 0.439, 2.413, respectively, and 7.049 $mV\,cm$ for polynomials of degree 3 (the space between the nodes was kept at 20 μm). To give an example of the order of magnitude we are dealing with, errors of 24.7 and 59.1 $mV\,cm$ are associated with a phase shifts of 0.1 and 0.5 msec, respectively. On should note in panel B of Figure 1 that, for the selected parameters, polynomials of degree 1 were more accurate than polynomials of degree 3. This is because, a coarse discretization in space produces a phase delay while a large time step produces a phase advance. For this particular case, there was stronger cancellation of these errors with polynomials of degree 1. In addition, we observed that polynomials of high degree should be used with care. If there are not enough elements, the polynomial interpolation can develop oscillations between the nodes and lead to a dramatic degradation in accuracy.

Self-sustaining spiral wave

We modified the LR model as follows: i) we shifted by 10 mV the steady state of the sodium current gates, ii) we added an offset of 0.16 msec to the time constant of the activation gate of the sodium current; iii) we divided the maximal conductance of the slow inward current by 2; iv) we replaced the delayed rectifier current by the Matsuura formulation [9]; and iv) we by multiplied the conductance of the inward rectifier by 2. This model exhibited an APD of 220 msec; a refractory period of 231 msec, and a propagation velocity of 33 cm/sec (wavelength 7.6 cm). The model reproduced well the characteristics of planar wave as measured on small preparations. Using this model we initiated a spiral wave in a uniform isotropic sheet of 4 cm x 4 cm using cross field stimulation. The axial resistivity was constant at 200 Ωcm, which is comparable to the longitudinal axial resistivity of the cardiac fibers [6]. The numerical solution was computed using 400 elements with polynomials of degree 1 and a time step of 0.1 msec. An "electrode" (E1) of 2 mm x 4 cm was placed vertically on the left side of the cardiac sheet. Another electrode (E2) was placed on the lower left quadrant of the cardiac sheet. The size of (E2) was 2 cm x 1.6 cm. The stimulus amplitude for the cross field stimulation was 1.5 and 3 times threshold for S1 and S2, respectively; in both cases the stimulus duration was 5 msec. The threshold was determined as the minimum stimulus amplitude which generated a propagated response. Figure 2 depicts the spatial distribution of membrane

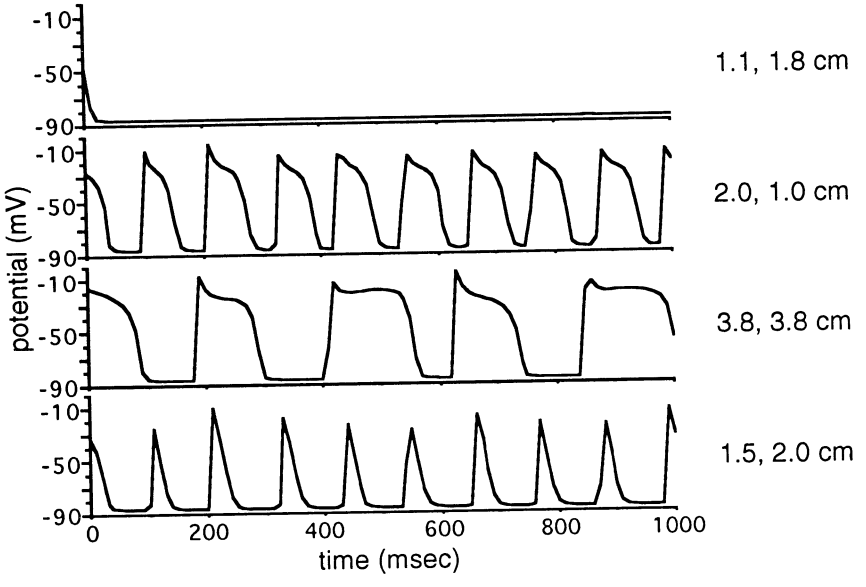


Figure 3: Membrane potential in time during spiral wave activity (see text for details).

voltage during spiral wave activity in a window of time ranging from 820 to 960 msec after application of S2. The excitation pattern was sustained and stable, as suggested by a continuous 1-sec recording of a spiral rotating at a period of $\approx$ 115 msec. The coordinates of the center of rotation were 1.1, 1.8 cm from the lower right corner (reference point) of the matrix. The tip of the spiral meandered around this center of rotation.

It is of interest that although there was only one excitation source throughout the simulation, the local patterns of electrical activity seemed disorganized, as shown by the recordings presented in Figure 3. The membrane potential within the area of 0.9 to 1.3 cm longitudinally, and 1.6 to 2.0 cm transversely with respect to the lower right corner never depolarized above -75 mV. This demonstrated that the organizing center of the spiral wave activity, which was located in that region, was never excited. Near the core, cells fully depolarized periodically by the rotating waves, which established gradients of membrane potential with respect to cells within the core. This produced large axial current flow which accelerated repolarization of the action potentials generated around the core, and resulted in a radial gradient of action potential duration (APD). Such a gradient may be appreciated by comparing the individual recordings presented in Figure 3. One important consequence of the APD gradient was the prolongation of the refractory period in the periphery of the matrix, which set the stage for interactions between the wave front and the wave tail, and established a 2:1 excitation pattern near the upper and lower borders of the array (see second

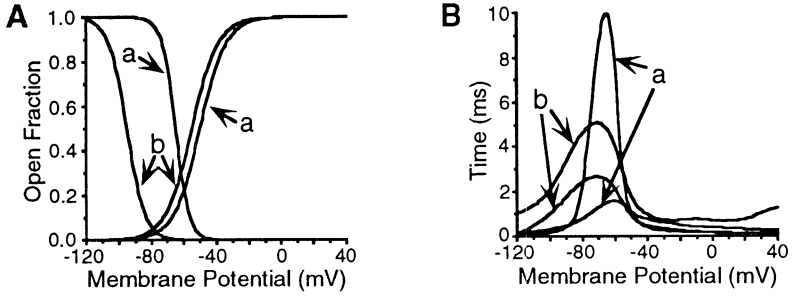


Figure 4: Steady state (A) and time constant (B) of two different current model extracted from patch clamp data of Murray's et al.

trace from the bottom in Figure 3). In Figure 2, a reduction of the space separating the wave front and the wave tail can be observed near the upper left border between the frames taken at 880 msec and 920 msec. Subsequently, between 920 and 960 msec, decremental propagation ensued in that region, leading to conduction block. Hence because of the large excitable space that remained after termination of this wave (upper left portion of frame 960 msec) the subsequent rotating impulse could propagate through that region without decrement.

Revision of the sodium current

The important modification which enabled us to realistically reproduce spiral wave activity in such a small matrix was an increase in threshold by 10 mV and an offset of the activation and inactivation time constant of 0.16 msec. This suggested an important role for the sodium current kinetics in the establishment of sustained spiral wave activity. Therefore, We examined the most recently published results on the sodium current in isolated myocytes [10] to extract current model parameters and revise the kinetics of the activation front of the existing membrane model.

Extracting the current model parameters from patch-clamp data is a difficult task. There is still no theory that guarantees the estimation of a unique set of parameters from the nonlinear model response. Faced with this situation, parameter estimation for a particular model should be the object of a specific study. A theory has previously been developed for the estimation of HH model parameters [3, 2]. In the latter it was demonstrated that simply using two voltage clamp stimulation protocols where the holding and test potentials are varied to obtain the peak current provides insufficient information for extracting a unique parameter set. In [2] it was demonstrated that a set of 4 complementary stimulation protocols can provide optimal data to extract a unique set of parameters. However, in the particular case where the activation and inactivation time constants are far apart from each other, two conventional protocols provide enough

information to identify a unique parameter set [3]. We applied the parameter estimation procedure [3] to the patch clamp data obtained by Murray et al [10] and found that the time constants are too close to each other, which precluded application of this theory. The steady state and time constants of two different current models are shown in Figure 4. The model response to voltage clamp stimulation for these two models are compared with the experimental results of Murray [10] in Figure 5. Panel (A) shows the Ipeak(V) relations obtained using a voltage clamp protocol when the holding and test potentials are varied. Panel (B) shows the time to peak when the test potential is varied. In panels (C) and (D) we show the current traces in time. They are similar to the experimental traces of Murray et al [10]. For models a and b, $\bar{g}_{Na}$=42.5 and 4.27 nS. For each model E_{Na}=39 mV. Either of these two models reproduces very well the experimental data used to estimate the parameters. It should be noted that, in addition to a slight deviation in the current traces in time after 0.4 msec, the model responses are quite similar and simulate closely the experimental data. However these two models are different (see Figure 3) and can produce very different responses under different conditions of stimulation. For example, we compared the cell response to a current stimulus when the sodium current of the LR model was replaced by either of the models presented in Figure 3. While one model predicted a normal action potential, the other predicted (which is obviously erroneous) no repolarization. For one of the models, there was a large conductance window (i.e., a large range of potentials in which the product of the activation and inactivation gates was significant). This model predicted a large window current during repolarization which is not present in the other model. The latter is responsible for the failure to repolarize.

4 Discussion

An extensive revision of the kinetics of the membrane currents of the ventricular cells has been provided by Luo and Rudy and integrated in a membrane model [8]. We did not attempt to verify whether or not this model can realistically reproduce spiral wave activity. We were concerned primarily with developing a theory that would enable us to incorporate in a membrane model current kinetics obtained in patch-clamp experiments. Our rationale was that this approach would eventually lead us to mimic a large variety of conditions occurring during cardiac arrhythmias. In this study we examined how one can modify the kinetics of the activation front by modifying the sodium current. This exercise illustrated well some of the problems one must deal with when constructing a membrane model. Given a mathematical formulation (or structure) for a current model, which describes its kinetics, one has to determine how to generate the minimum required information to obtain a unique set of parameters. In the current case we

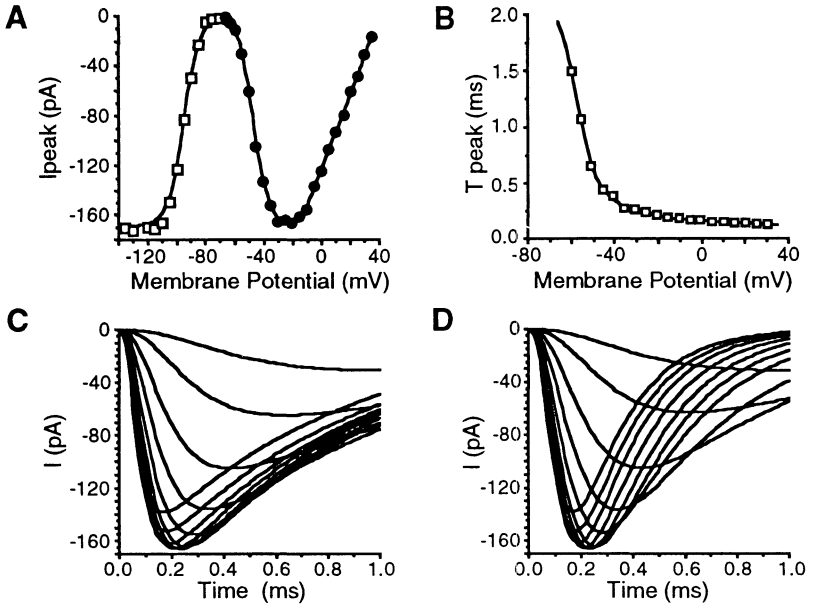


Figure 5: Comparison of model response (solid line) with experimental data (symbols). See text for details. Experimental data were reproduced from the paper by Murray's et al [10] with the permission of the author and the editor.

demonstrated that the patch-clamp data (peak currents and time to peak) provided by two voltage clamp stimulation protocols were not sufficient to characterize the kinetics of a current in the context of construction of an action potential model. Consequently, the approach did not enable us to revise the kinetics of the activation front of the electrical impulse. This is an important point because it applies to any current of the membrane model and also to the characterization of the effects of drugs and other ministrations on the membrane dynamics. In [2] it was proposed that a set of 4 complementary stimulation protocols provide an optimal data set for the parameter estimation of a HH type current model. Unfortunately, it appears that, in practice (at least in most of the cases), no significant amplitude can be obtained for certain stimulation protocols. The determination of stimulation protocols which will provide an optimal data set for the characterization of the current kinetic is the subject of an ongoing study in our laboratory.

References

[1] Axelsson O., Barker V.A. *Finite Element Solution of Boundary Value Problems.* Academic Press Inc., 1984.

[2] Beaumont J., Roberge F.A., Lemieux D.R. Estimation of the steady-state characterisitcs of the hodgkin-huxley model from voltage clamp data. *Math. Biosciences*, 11:145–186, 1993.

[3] Beaumont J., Roberge F.A., Leon L.J. On the interpretation of voltage-clamp data using the hodgkin-huxley model. *Math. Biosciences*, 115:65–101, 1993.

[4] Courtemanche M., Winfree A. Re-entrant rotating waves in a beeler-reuter based model of two dimensional cardiac electrical activity. *Int. J. Bifurc. and Chaos*, 1:431–444, 1991.

[5] Davidenko JM, Kent P., Chialvo DR. Michaels DC. Sustained vortex-like waves in normal isolated ventricular muscle. *Proc. Natl. Acad. Sci. USA*, 87:8785–8789, 1990.

[6] Leon LJ., Roberge FA., Vinet A. Simulation of two-dimensional anisotropic cardiac reentry: effects of the wavelength on the reentry characterisitcs. *Annals of biomed. Eng.*, 22:6, 1994.

[7] Luo C.R., Rudy Y. A model of ventricular cardiac action potential: depolarization, repolarization and their interaction. *Circ. res.*, 68:1501–1526, June 1991.

[8] Luo C.R., Rudy Y. A dynamic model of the cardiac ventricular action potential: I, simulations of ionic currents and concentration changes. *Circ. Res.*, 76(6):1071–1096, 1994.

[9] Matsuura H., Ehara T., Imoto Y. An analysis of the delayed outward current in single ventricular cells of the guinea-pig. *Pflugers Arch.*, 410:596–603, 1987.

[10] Murray K.T., Anno T., Bennett P.B., Hondeghem L.M. Voltage clamp of the cardiac sodium current at $37^0\,c$ in physiologic conditions. *Biophysical J.*, 57:607–613, 1990.

[11] Reddy J.N. *An Introduction to the Finite Element Method.* Mc Graw-Hill Publishing Company, 1984.